



# DIGITAL ACCESS TO SCHOLARSHIP AT HARVARD

## Neprilysin Deficiency Protects Against Fat-Induced Insulin Secretory Dysfunction by Maintaining Calcium Influx

The Harvard community has made this article openly available.  
[Please share](#) how this access benefits you. Your story matters.

<b>Citation</b>	Zraika, Sakeneh, Duk-Su Koh, Breanne M. Barrow, Bao Lu, Steven E. Kahn, and Sofianos Andrikopoulos. 2013. "Neprilysin Deficiency Protects Against Fat-Induced Insulin Secretory Dysfunction by Maintaining Calcium Influx." <i>Diabetes</i> 62 (5): 1593-1601. doi:10.2337/db11-1593. <a href="http://dx.doi.org/10.2337/db11-1593">http://dx.doi.org/10.2337/db11-1593</a> .
<b>Published Version</b>	<a href="https://doi.org/10.2337/db11-1593">doi:10.2337/db11-1593</a>
<b>Accessed</b>	February 16, 2015 1:03:28 PM EST
<b>Citable Link</b>	<a href="http://nrs.harvard.edu/urn-3:HUL.InstRepos:12407011">http://nrs.harvard.edu/urn-3:HUL.InstRepos:12407011</a>
<b>Terms of Use</b>	This article was downloaded from Harvard University's DASH repository, and is made available under the terms and conditions applicable to Other Posted Material, as set forth at <a href="http://nrs.harvard.edu/urn-3:HUL.InstRepos:dash.current.terms-of-use#LAA">http://nrs.harvard.edu/urn-3:HUL.InstRepos:dash.current.terms-of-use#LAA</a>

*(Article begins on next page)*

# Neprilysin Deficiency Protects Against Fat-Induced Insulin Secretory Dysfunction by Maintaining Calcium Influx

Sakeneh Zraika,<sup>1</sup> Duk-Su Koh,<sup>2</sup> Breanne M. Barrow,<sup>1</sup> Bao Lu,<sup>3</sup> Steven E. Kahn,<sup>1</sup> and Sofianos Andrikopoulos<sup>4</sup>

Neprilysin contributes to free fatty acid (FFA)-induced cellular dysfunction in nonislet tissues in type 2 diabetes. Here, we show for the first time that with prolonged FFA exposure, islet neprilysin is upregulated and this is associated with reduced insulin pre-mRNA and ATP levels, oxidative/nitrative stress, impaired potassium and calcium channel activities, and decreased glucose-stimulated insulin secretion (GSIS). Genetic ablation of neprilysin specifically protects against FFA-induced impairment of calcium influx and GSIS in vitro and in vivo but does not ameliorate other FFA-induced defects. Importantly, adenoviral overexpression of neprilysin in islets cultured without FFA reproduces the defects in both calcium influx and GSIS, suggesting that upregulation of neprilysin per se mediates insulin secretory dysfunction and that the mechanism for protection conferred by neprilysin deletion involves prevention of reduced calcium influx. Our findings highlight the critical nature of calcium signaling for normal insulin secretion and suggest that interventions to inhibit neprilysin may improve  $\beta$ -cell function in obese humans with type 2 diabetes. *Diabetes* 62:1593–1601, 2013

**F**undamental to development of type 2 diabetes is failure of  $\beta$ -cells to secrete adequate amounts of insulin in order to maintain blood glucose levels within the normal range (1). A common feature of type 2 diabetes is obesity and concomitantly elevated free fatty acid (FFA) levels (2). It has long been recognized that elevated FFAs have differential effects on insulin secretion depending on duration of exposure; acute exposure leads to increased insulin secretion (3,4), while chronic exposure impairs insulin secretion and results in  $\beta$ -cell death (5,6).

Chronically elevated FFAs induce defects at multiple steps in the pathways governing insulin production and secretion. As palmitate is a predominant fatty acid in human plasma and is increased in obese individuals (7), its use in studies of  $\beta$ -cell function has relevance for human disease. Studies have shown that palmitate inhibits glucose-induced

insulin promoter activity leading to suppression of insulin gene expression (8). Key enzymes in glucose and lipid metabolism are also dysregulated by palmitate exposure (9), leading to mitochondrial defects such as reduced ATP production (10) and induction of oxidative/nitrative stress (11,12). In addition, dysregulated calcium homeostasis (13,14) and soluble *N*-ethylmaleimide-sensitive factor attachment protein receptor (SNARE) complex assembly and/or expression (15,16) due to chronic FFAs have been reported. Thus, while numerous FFA-induced  $\beta$ -cell defects have been demonstrated, the critical cellular mediators that contribute to reduced insulin secretion remain incompletely defined.

Neprilysin is a widely expressed plasma membrane protein that in nonislet tissues (e.g., mesenteric fat, endothelium) is upregulated under conditions of elevated FFAs and has been postulated to mediate cellular dysfunction in type 2 diabetes (17–19). We recently demonstrated that neprilysin is synthesized in islets (20) and could therefore play a role in FFA-induced islet dysfunction. Its normal function depends on the tissue in which it is located, where it can exert effects via its dual activities: proteolysis (21) or protein binding (22–24). Typical functions comprise metabolism of various regulatory peptides of the nervous, cardiovascular, and immune systems (25). Functions relevant to the islet include involvement in various signaling pathways including the IGF receptor–Akt cell survival pathway (23,24,26), degradation of peptides like glucagon and glucagon-like peptide-1 (27), inhibition of islet amyloid formation (20,28), and being a component of the renin-angiotensin system (29,30). The contribution of islet neprilysin to insulin secretory (dys)function has not previously been investigated.

Given the central role of the islet in regulating glucose homeostasis and evidence that upregulation of neprilysin may be deleterious to cellular function, we sought to determine whether islet neprilysin contributes to FFA-induced insulin secretory dysfunction by studying the impact of neprilysin deficiency on insulin secretion after chronic exposure to palmitate in vitro and high-fat feeding in vivo.

From the <sup>1</sup>Department of Medicine, VA Puget Sound Health Care System and University of Washington, Seattle, Washington; the <sup>2</sup>Department of Physiology and Biophysics, University of Washington, Seattle, Washington; the <sup>3</sup>Department of Pediatrics, Children's Hospital, Harvard Medical School, Boston, Massachusetts; and the <sup>4</sup>Department of Medicine, Heidelberg Repatriation Hospital, University of Melbourne, Heidelberg Heights, Victoria, Australia.

Corresponding author: Sakeneh Zraika, zraikas@u.washington.edu. Received 14 November 2012 and accepted 2 December 2012.

DOI: 10.2337/db11-1593

This article contains Supplementary Data online at <http://diabetes.diabetesjournals.org/lookup/suppl/doi:10.2337/db11-1593/-/DC1>.

© 2013 by the American Diabetes Association. Readers may use this article as long as the work is properly cited, the use is educational and not for profit, and the work is not altered. See <http://creativecommons.org/licenses/by-nc-nd/3.0/> for details.

## RESEARCH DESIGN AND METHODS

Breeding pairs of neprilysin-deficient mice on a C57BL/6 background (C57BL/6.NEP<sup>-/-</sup>) were provided by Dr. B. Lu, Department of Pediatrics, Children's Hospital, Harvard Medical School, Boston, Massachusetts (31), and a colony was established both in Seattle, Washington, for in vitro studies and in Melbourne, Australia, for in vivo studies. Age-matched C57BL/6J wild-type mice from The Jackson Laboratory were used as controls. For ensuring suitability of C57BL/6J mice as controls, C57BL/6.NEP<sup>+/-</sup> littermate mice were generated for confirmation experiments. Studies were approved by the VA Puget Sound Health Care System Institutional Animal Care and Use Committee in Seattle and the Austin Health Animal Ethics Committee in Melbourne.

**Islet isolation and culture.** Islets were isolated from 10-week-old female and male mice as previously described (32). After overnight recovery, islets were transferred to RPMI media containing 11.1 mmol/L glucose plus either 1 mmol/L palmitate complexed to BSA in a 5:1 molar ratio or vehicle mixed with fatty acid-free BSA and cultured for 48 h. For adenovirus studies, freshly isolated islets were infected with  $2.1 \times 10^6$  pfu/mL (multiplicity of infection = 13) adenovirus containing either green fluorescent protein (AdV-GFP) (gift from Dr. C. Rhodes, Department of Medicine, University of Chicago, Chicago, IL) or neprilysin (AdV-NEP) (gift from Dr. J. Robbins, Molecular Cardiovascular Biology, Cincinnati Children's Hospital, Cincinnati, OH) cDNA for 20 h, transferred to media containing 11.1 mmol/L glucose, and cultured for 48 h. AdV-GFP and AdV-NEP are similar in construction, prepared using Stratagene's AdEasy system (La Jolla, CA).

**Real-time quantitative RT-PCR.** Expression of neprilysin mRNA and insulin pre-mRNA was determined with real-time quantitative RT-PCR using TaqMan (Mm00485028\_m1; Applied Biosystems, Carlsbad, CA) and SYBR Green (Eurofins MWG Operon, Huntsville, AL) systems, respectively. TaqMan eukaryotic 18S rRNA (Hs99999901\_s1; Applied Biosystems) was used as endogenous control.

**Neprilysin enzymatic activity assay.** Islet neprilysin enzyme activity was determined fluorometrically as previously described (20), with kidney as a positive control. Briefly, glutaryl-ala-ala-phe-4-methoxy-2-naphthylamine is broken down by neprilysin in lysates to Phe-4-methoxy-2-naphthylamine and then the fluorescent product methoxy-2-naphthylamine by aminopeptidase M. The specific neprilysin inhibitor DL-thiorphan differentiates neprilysin activity from nonspecific endopeptidase activity. Fluorescence is compared against a methoxy-2-naphthylamine standard curve. C57BL/6.NEP<sup>-/-</sup> islets had undetectable neprilysin activity levels ( $n = 4$ ).

**Insulin secretion and content.** Insulin secretion in response to 2.8 mmol/L (basal) or 20 mmol/L (stimulated) glucose was measured in static incubations as previously described (32). Islet insulin content was measured after acid-ethanol extraction. Insulin concentrations were determined using the Insulin (Mouse) Ultrasensitive ELISA (Alpco, Salem, NH).

**ATP and nitrate/nitrite levels.** Islet ATP levels at 2.8 and 20 mmol/L glucose were determined as previously described (32) using an ATP bioluminescent assay kit (Sigma, St. Louis, MO). Forty-eight h conditioned medium was collected and assayed for nitrate and nitrite using a colorimetric kit (Cayman Chemical, Ann Arbor, MI).

**Western blotting.** Islet protein separated by SDS-PAGE was transferred to polyvinylidene fluoride membranes, which were probed with polyclonal rabbit anti-neprilysin (1:200; Santa Cruz Biotechnology, Santa Cruz, CA) or polyclonal mouse anti-nitrotyrosine (1:1,000; Millipore, Billerica, MA) antibodies. Stripped membranes were reprobed with rabbit anti- $\beta$ -actin (1:2,000; Sigma) antibody as a loading control. Secondary antibodies were goat anti-rabbit (1:100,000; Dako, Carpinteria, CA) and goat anti-mouse (1:100,000; Pierce, Rockford, IL) IgG coupled to horseradish peroxidase.

**Rubidium efflux.** K<sup>+</sup> permeability of islets was measured in static incubations by monitoring of <sup>86</sup>Rb<sup>+</sup> efflux. Briefly, islets were incubated for 90 min with <sup>86</sup>RbCl (50  $\mu$ Ci/mL), washed four times, and then incubated with 2.8 and 20 mmol/L glucose for 20 min. Incubations with 1  $\mu$ mol/L glyburide or 500  $\mu$ mol/L diazoxide were performed as controls for decreased and increased <sup>86</sup>Rb<sup>+</sup> efflux, respectively. <sup>86</sup>Rb<sup>+</sup> in supernatant and islet fractions was measured by liquid scintillation counting and fractional efflux calculated.

**Calcium influx and imaging.** Calcium influx in the presence of 2.8 or 20 mmol/L glucose was measured as previously described (33). As a control, a subset of islets was incubated in 20 mmol/L glucose plus the calcium channel blocker nimodipine (5  $\mu$ mol/L).

Calcium imaging of islets loaded with 4  $\mu$ mol/L fluo-4 AM or 30  $\mu$ mol/L Rhod-3 AM for 30 min and perfused with 2.8 or 20 mmol/L glucose was performed with a laser-scanning confocal microscope (Zeiss LSM 510 META). Rhod-3 was used only in adenovirus-infected islets, since fluo-4 overlaps spectrally with GFP. Changes in intracellular calcium concentrations were measured as changes in emission intensity at 500–550 nm (fluo-4) or 600–700 nm (Rhod-3) upon excitation with 488-nm (fluo-4) or 561-nm (Rhod-3) lasers. Images were acquired at 10-s intervals, and average fluorescence intensity per islet was calculated using ImageJ software (NIH Image, Bethesda, MD). As a result of high spatial resolution, confocal imaging allows for detection of calcium levels in individual cells. Thus, the percentage of cells responding to 20 mmol/L glucose (determined as an increment in fluorescence above basal) relative to the total number of cells per islet was computed for an average of 14 islets/condition.

**High-fat feeding and in vivo assessments.** Ten-week-old C57BL/6.NEP<sup>-/-</sup> and C57BL/6 female and male mice were assigned to receive either standard rodent chow containing (w/w) 3% fat, 20% protein, and 77% carbohydrate or high-fat diet containing (w/w) 60% fat, 18% protein, and 22% carbohydrate (Ridley AgriProducts, Pakenham, Victoria, Australia). After 12 weeks of feeding, body weights were determined and intravenous glucose (IVGTTs) (1 g/kg) or intraperitoneal insulin (IPITTs) (0.75 IU/kg) tolerance tests performed with plasma glucose and insulin measured as previously described

(34). No differences were observed in glucose or insulin measures between female and male mice, and thus data from both sexes were pooled. In a cohort of nonfasted C57BL/6 mice, plasma was obtained after 8 weeks of feeding for determination of FFA levels using the Wako NEFA-C kit (Wako Chemicals, Richmond, VA). At the conclusion of tolerance testing, pancreata were excised and paraffin embedded for histological assessment of insulin and glucagon as previously described (20).

**Statistical analyses.** Data are presented as means  $\pm$  SEM for the number of experiments indicated. Statistical significance was determined using ANOVA with post hoc analysis or Mann-Whitney *U* test if data were not normally distributed. A  $P < 0.05$  was considered statistically significant.

## RESULTS

**Neprilysin activity is upregulated with chronic palmitate exposure.** We first determined whether islet neprilysin levels are increased with chronic FFA exposure as in other tissues (18,35). After 48-h culture of C57BL/6 mouse islets in the absence versus presence of palmitate, neprilysin mRNA (Fig. 1A) and protein (Fig. 1B) levels were unchanged, whereas neprilysin activity (Fig. 1C) was elevated 1.6-fold.

**Neprilysin deficiency provides selective protection against palmitate-induced reductions in glucose-stimulated insulin secretion.** Insulin secretion under basal conditions (2.8 mmol/L glucose) and in response to glucose stimulation (20 mmol/L glucose) was assessed after 48-h culture of islets in the absence and presence of palmitate (Fig. 2A). In C57BL/6 islets, palmitate exposure increased basal and decreased glucose-stimulated insulin secretion (GSIS) as expected. In C57BL/6.NEP<sup>-/-</sup> islets exposed to palmitate, basal insulin secretion was also increased. In contrast, GSIS was not decreased after chronic palmitate exposure in C57BL/6.NEP<sup>-/-</sup> islets. This same pattern of insulin secretion was also observed in cultured islets from C57BL/6.NEP<sup>+/+</sup> and C57BL/6.NEP<sup>-/-</sup> littermates (Supplementary Fig. 1).

Islet insulin content (Fig. 2B) and pre-mRNA levels (Fig. 2C) were measured and found to be decreased after palmitate exposure in both C57BL/6 and C57BL/6.NEP<sup>-/-</sup> islets, indicating that protection conferred by neprilysin deficiency was not mediated by preventing palmitate-induced decreases in insulin biosynthesis but, rather, was selective for GSIS. Total protein content of islets from C57BL/6 and C57BL/6.NEP<sup>-/-</sup> mice did not differ ( $0.20 \pm 0.02$  vs.  $0.18 \pm 0.02$   $\mu$ g protein/islet for  $105 \pm 7$  islets/mouse from 33 mice/genotype).

**Neprilysin deficiency does not protect against palmitate-induced reductions in ATP levels or production of nitric oxide and peroxynitrite.** For determination of the mechanism for protection against reduced GSIS in neprilysin-deficient islets, ATP levels were assessed after 48-h cultures (Fig. 3A). As expected in C57BL/6 and C57BL/6.NEP<sup>-/-</sup> islets cultured in the absence of palmitate, ATP levels increased with 20 mmol/L glucose relative to 2.8 mmol/L glucose. In contrast, C57BL/6 islets exposed to palmitate had significantly reduced ATP levels with 20 mmol/L glucose. Similarly, C57BL/6.NEP<sup>-/-</sup> islets exposed to palmitate had reduced ATP levels with 20 mmol/L glucose.

Since FFA-induced oxidative/nitrative stress can adversely affect  $\beta$ -cell stimulus-secretion coupling (11,12), nitric oxide and nitrotyrosine (a marker for peroxynitrite) were measured to determine whether reduced oxidative/nitrative stress in palmitate cultured C57BL/6.NEP<sup>-/-</sup> islets could explain the absence of a GSIS defect. Figure 3B shows increased nitrate levels from islets exposed to palmitate, regardless of genotype. Similarly, nitrotyrosine levels assessed by immunoblotting were elevated in islets exposed to palmitate, regardless of genotype (data not shown).

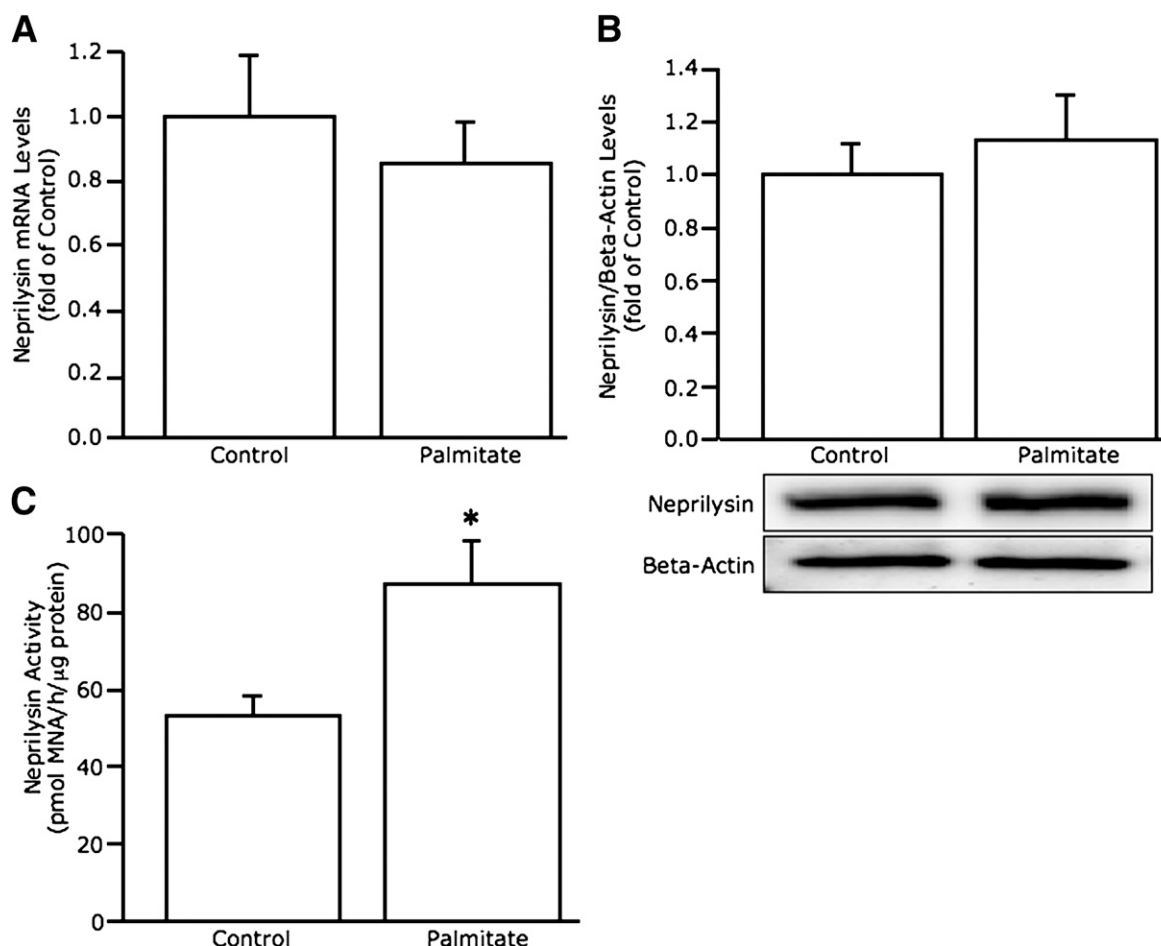


FIG. 1. Palmitate exposure increases neprilysin activity but not mRNA or protein levels in C57BL/6 islets. Neprilysin mRNA expression (A) ( $n = 11$ ), protein levels (B) ( $n = 6$ ; image is a representative blot), and activity (C) ( $n = 5$ ) in C57BL/6 islets after 48-h culture in the absence or presence of 1 mmol/L palmitate. Data are means  $\pm$  SEM. \* $P = 0.02$  vs. control.

### Calcium but not potassium channel activity is involved in protecting neprilysin-deficient islets from palmitate-induced insulin secretory dysfunction.

As neprilysin has been suggested to modulate potassium and calcium ion flux in nonislet tissues (36,37), we investigated whether neprilysin may play a similar role in islets, thereby mediating palmitate-induced defects. Rubidium efflux, reflecting  $K^+$  permeability, decreased in response to 20 mmol/L glucose relative to 2.8 mmol/L glucose in both C57BL/6 and C57BL/6.NEP<sup>-/-</sup> islets cultured in the absence of palmitate (Fig. 4). In the presence of palmitate, rubidium efflux in response to 20 mmol/L glucose was increased in C57BL/6 and C57BL/6.NEP<sup>-/-</sup> islets compared with islets cultured in the absence of palmitate, suggesting that neprilysin's site of action is likely distal to the potassium channel. Diazoxide, an opener, and glyburide, a blocker of  $K_{ATP}$  channels, were used as controls for increased and decreased rubidium efflux, respectively; no differences were observed between genotypes (diazoxide with 20 mmol/L glucose, C57BL/6  $3.3 \pm 0.4\%$   $^{86}Rb^+$ /min vs. C57BL/6.NEP<sup>-/-</sup>  $2.8 \pm 0.1\%$   $^{86}Rb^+$ /min; glyburide with 2.8 mmol/L glucose, C57BL/6  $1.9 \pm 0.1\%$   $^{86}Rb^+$ /min vs. C57BL/6.NEP<sup>-/-</sup>  $1.9 \pm 0.1\%$   $^{86}Rb^+$ /min;  $n = 5$ ).

Influx of radiolabeled calcium ( $^{45}Ca^{2+}$ ) into islet cells was increased in response to 20 mmol/L glucose relative to 2.8 mmol/L glucose in both C57BL/6 and C57BL/6.NEP<sup>-/-</sup> islets cultured in the absence of palmitate (Fig. 5A). In C57BL/6 islets cultured in the presence of palmitate,

calcium influx in response to 20 mmol/L glucose was decreased. In contrast, in C57BL/6.NEP<sup>-/-</sup> islets cultured in the presence of palmitate, calcium influx in response to 20 mmol/L glucose remained unchanged compared with islets in the absence of palmitate. Nimodipine, an L-type calcium channel blocker, was used as a control in calcium influx studies. While nimodipine in the presence of 20 mmol/L glucose blocked calcium influx as expected, no difference was observed between genotypes (C57BL/6  $3.6 \pm 0.7$  pmol/min vs. C57BL/6.NEP<sup>-/-</sup>  $4.0 \pm 0.4$  pmol/min;  $n = 5$ ).

For confirmation that neprilysin deficiency was indeed protecting islets exposed to palmitate from reduced glucose-stimulated calcium influx, the more sensitive and real-time measure of calcium imaging using fluo-4 was used. Representative calcium imaging traces (Fig. 5B) clearly show that C57BL/6.NEP<sup>-/-</sup> islets are protected from the effects of palmitate exposure to inhibit glucose-induced calcium influx. Mean data from fluo-4 experiments are expressed as the proportion of islet cells that responded (i.e., displayed enhanced fluorescence) to treatment with 20 mmol/L glucose (Fig. 5C). In C57BL/6 and C57BL/6.NEP<sup>-/-</sup> islets cultured in the absence of palmitate, 37 and 41% of islet cells, respectively, responded to 20 mmol/L glucose. In C57BL/6 islets cultured in the presence of palmitate, only 13% of islet cells responded to 20 mmol/L glucose. In contrast, in C57BL/6.NEP<sup>-/-</sup> islets cultured in the presence of palmitate, 31% of islet cells responded to

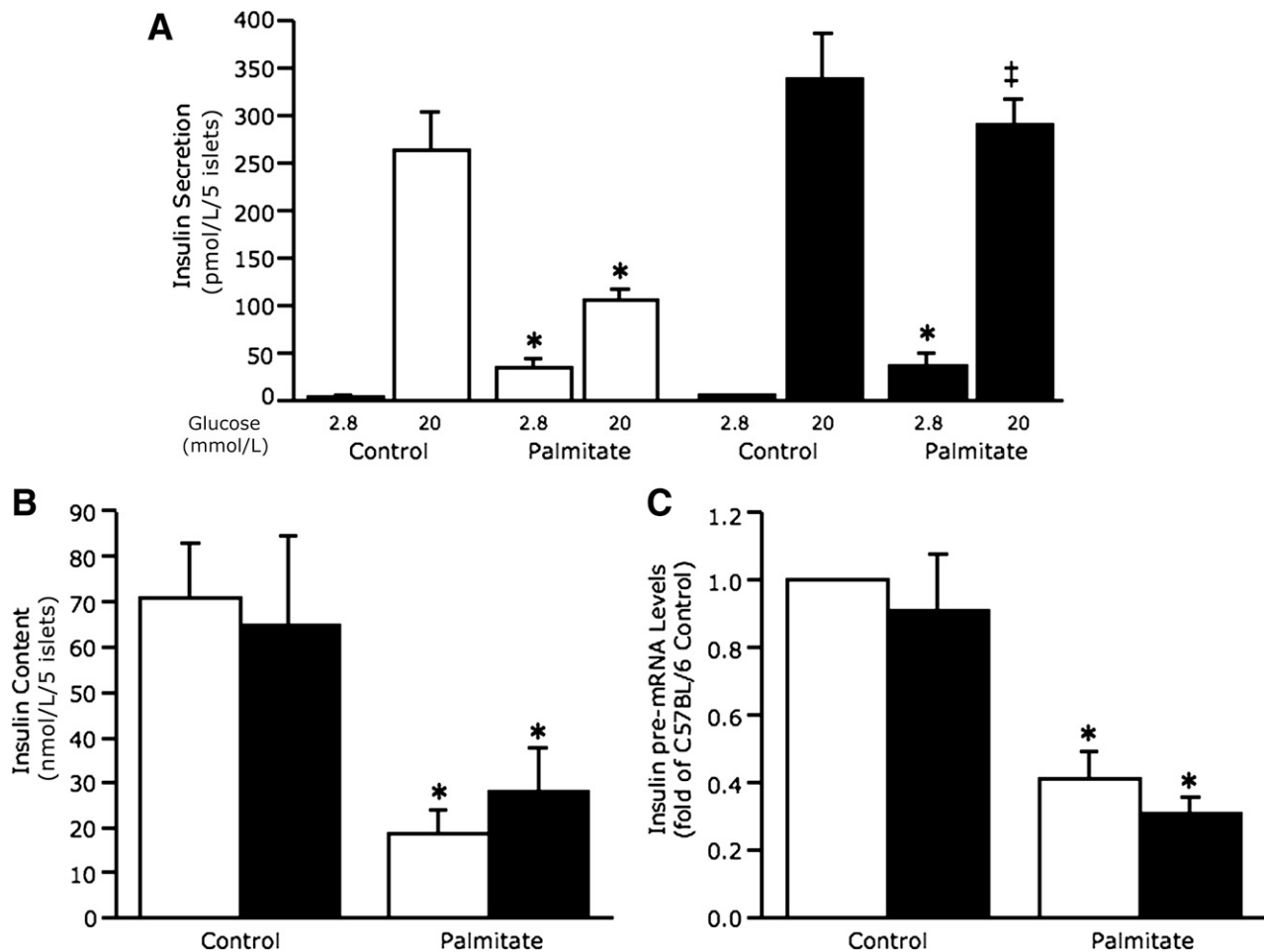


**FIG. 2.** Neprilysin-deficient islets are protected against palmitate-induced reductions in GSIS. Insulin secretion in response to 2.8 and 20 mmol/L glucose (*A*) ( $n = 5$ ), islet insulin content (*B*) ( $n = 5$ ), and insulin pre-mRNA levels (*C*) ( $n = 9$ ) from C57BL/6 and C57BL/6.NEP<sup>-/-</sup> islets after 48-h culture in the absence or presence of 1 mmol/L palmitate. White bars, C57BL/6 islets; black bars, C57BL/6.NEP<sup>-/-</sup> islets. Data are means  $\pm$  SEM. \* $P < 0.05$  vs. control; ‡ $P = 0.0001$  vs. C57BL/6.

20 mmol/L glucose. Thus, the fluo-4 imaging data corroborate the  $^{45}\text{Ca}^{2+}$  influx data, suggesting that neprilysin is involved in mediating FFA-induced insulin secretory dysfunction by inhibiting calcium influx.

**Upregulation of neprilysin in the absence of palmitate recapitulates the palmitate-induced impairment of GSIS.** Neprilysin was overexpressed in C57BL/6 islets to determine whether its upregulation is sufficient to inhibit calcium influx and reduce GSIS in the absence of palmitate. In AdV-NEP-infected islets, neprilysin protein and activity levels were increased  $5.3 \pm 1.8$ -fold and  $4.5 \pm 0.8$ -fold, respectively, versus control AdV-GFP-infected islets ( $n = 4-6$ ,  $P < 0.05$ ). Insulin secretion from both AdV-GFP- and AdV-NEP-infected islets was increased with 20 mmol/L glucose relative to 2.8 mmol/L glucose (Fig. 6A). However, in response to 20 mmol/L glucose, AdV-NEP-infected islets had significantly reduced insulin secretion compared with AdV-GFP-infected islets. Insulin content did not differ between AdV-GFP- and AdV-NEP-infected islets (Fig. 6B). Glucose-induced calcium influx was significantly reduced in AdV-NEP-infected versus AdV-GFP-infected islets (Fig. 6C).

**Neprilysin deficiency protects against high-fat diet-induced insulin secretory dysfunction in vivo.** High fat-fed C57BL/6 mice develop impaired GSIS in vivo

(38,39). For determination of whether neprilysin deficiency can protect against FFA-induced secretory dysfunction in vivo, C57BL/6 and C57BL/6.NEP<sup>-/-</sup> mice were fed a low- or high-fat diet for 12 weeks, after which insulin secretion and sensitivity were assessed by IVGTT and IPITT, respectively. Body weights (data not shown) and islet morphology (Supplementary Fig. 2) did not differ after 12 weeks of feeding regardless of genotype or diet. At 8 weeks, plasma FFA levels were higher in mice fed a high-versus low-fat diet ( $1.25 \pm 0.13$  vs.  $0.66 \pm 0.07$  mmol/L;  $n = 10$  mice/group,  $P < 0.001$ ). Despite the unexpected lack of weight gain, high-fat feeding had the expected effect of increasing fasting plasma glucose (Fig. 7A) and insulin (Fig. 7B) levels in both C57BL/6 and C57BL/6.NEP<sup>-/-</sup> mice. During the IVGTT, glucose levels were also elevated in mice fed a high-fat diet, with absolute levels at each time point being higher in C57BL/6.NEP<sup>-/-</sup> mice (Fig. 7C). However, glucose levels declined in parallel so that glucose tolerance, calculated as the glucose disappearance constant from 10 to 30 min, was comparable between high fat-fed C57BL/6 and C57BL/6.NEP<sup>-/-</sup> mice (high fat  $0.016 \pm 0.002$  vs.  $0.017 \pm 0.001\%$  per min; low fat  $0.018 \pm 0.001$  vs.  $0.022 \pm 0.001\%$  per min). The early insulin response (0–5 min) to glucose was reduced only in high fat-fed C57BL/6 mice (Fig. 7D). In contrast, the response in C57BL/6.NEP<sup>-/-</sup> mice

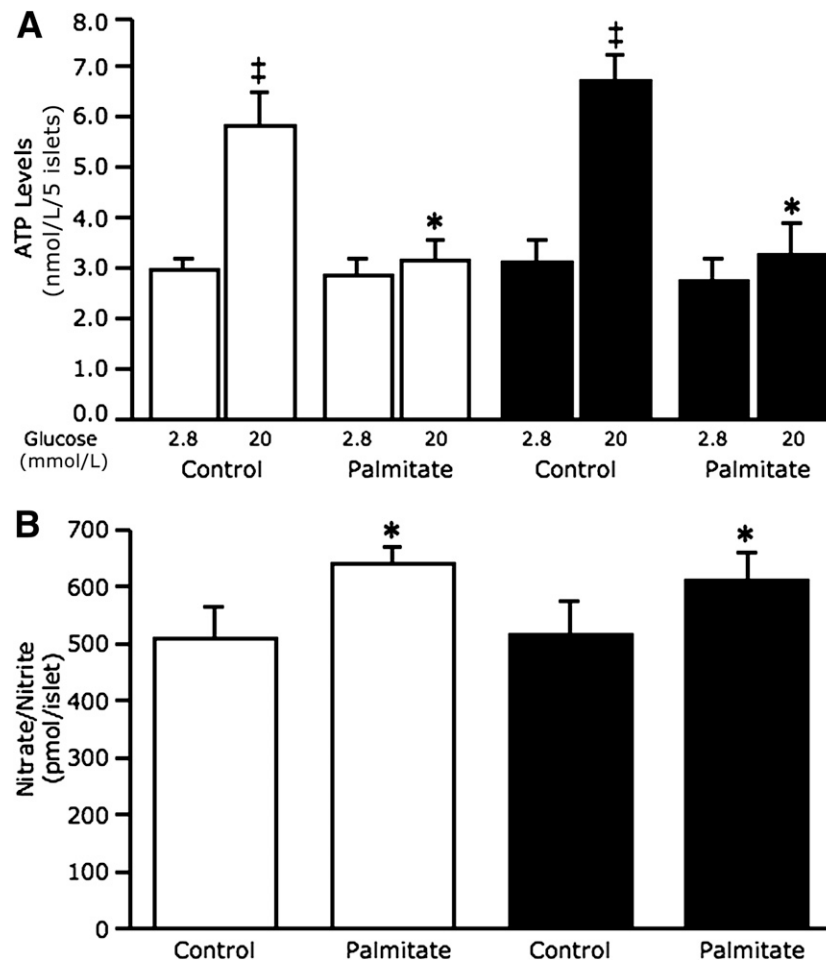


**FIG. 3.** Neprilysin-deficient islets exposed to palmitate are not protected against reduced glucose-stimulated ATP levels or nitrative stress. ATP levels in response to 2.8 and 20 mmol/L glucose stimulation (*A*) ( $n = 5$ ) and nitrate/nitrite levels (*B*) ( $n = 7$ ) from C57BL/6 and C57BL/6.NEP<sup>-/-</sup> islets after 48-h culture in the absence or presence of 1 mmol/L palmitate. White bars, C57BL/6 islets; black bars, C57BL/6.NEP<sup>-/-</sup> islets. Data are means  $\pm$  SEM. \* $P < 0.05$  vs. control; ‡ $P < 0.005$  vs. 2.8 mmol/L glucose.

fed a high-fat diet was increased and, when calculated in terms of the prevailing glucose level (Fig. 7*D*), remained unchanged compared with mice fed a low-fat diet. During the IPITT, glucose levels fell similarly in C57BL/6.NEP<sup>-/-</sup>

and C57BL/6 mice, though mice fed a low-fat diet were more insulin sensitive than mice fed a high-fat diet (Fig. 7*E*).

## DISCUSSION

Chronic elevations in circulating FFAs often accompany type 2 diabetes (2), and prolonged FFA exposure contributes to  $\beta$ -cell dysfunction (5,6). Neprilysin is a novel islet protein linked to FFA-induced cellular dysfunction in other tissues in type 2 diabetes (17). Here, we show for the first time that with prolonged FFA exposure, islet neprilysin activity is upregulated and this is associated with  $\beta$ -cell dysfunction. In addition, adenovirus-mediated overexpression of neprilysin in islets is sufficient to impair GSIS without exposure to FFAs. Importantly, genetic ablation of neprilysin protects against FFA-induced impairment of GSIS by preventing reduced calcium influx. These data suggest an important role for neprilysin in mediating GSIS, specifically by regulating calcium flux.

In  $\beta$ -cells chronically exposed to elevated FFAs, multiple defects contribute to increased basal insulin secretion, reduced GSIS, and reduced insulin content (40). We now report that palmitate-induced perturbations are associated with increased neprilysin activity, a finding documented in other tissues (18,35). In neprilysin-deficient islets, however, palmitate exposure failed to impair GSIS, suggesting that increased neprilysin activity contributes to palmitate-induced

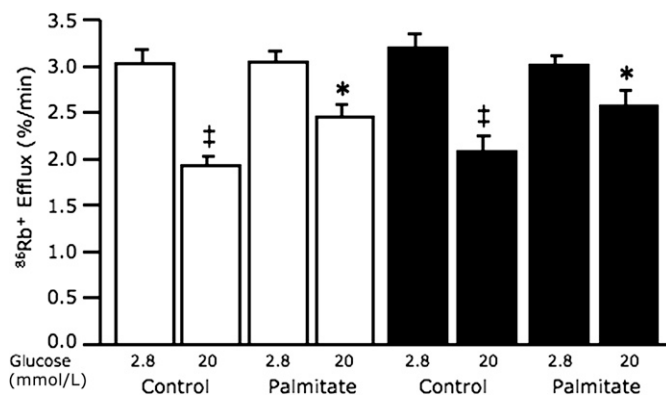


**FIG. 4.** Potassium efflux in response to 20 mmol/L glucose stimulation is similarly elevated in C57BL/6 and neprilysin-deficient islets after palmitate exposure. Rubidium efflux, reflecting K<sup>+</sup> permeability, in response to 2.8 and 20 mmol/L glucose stimulation from C57BL/6 and C57BL/6.NEP<sup>-/-</sup> islets after 48-h culture in the absence or presence of 1 mmol/L palmitate. White bars, C57BL/6 islets; black bars, C57BL/6.NEP<sup>-/-</sup> islets. Data are means  $\pm$  SEM;  $n = 5$ . \* $P < 0.05$  vs. control; ‡ $P < 0.001$  vs. 2.8 mmol/L glucose.

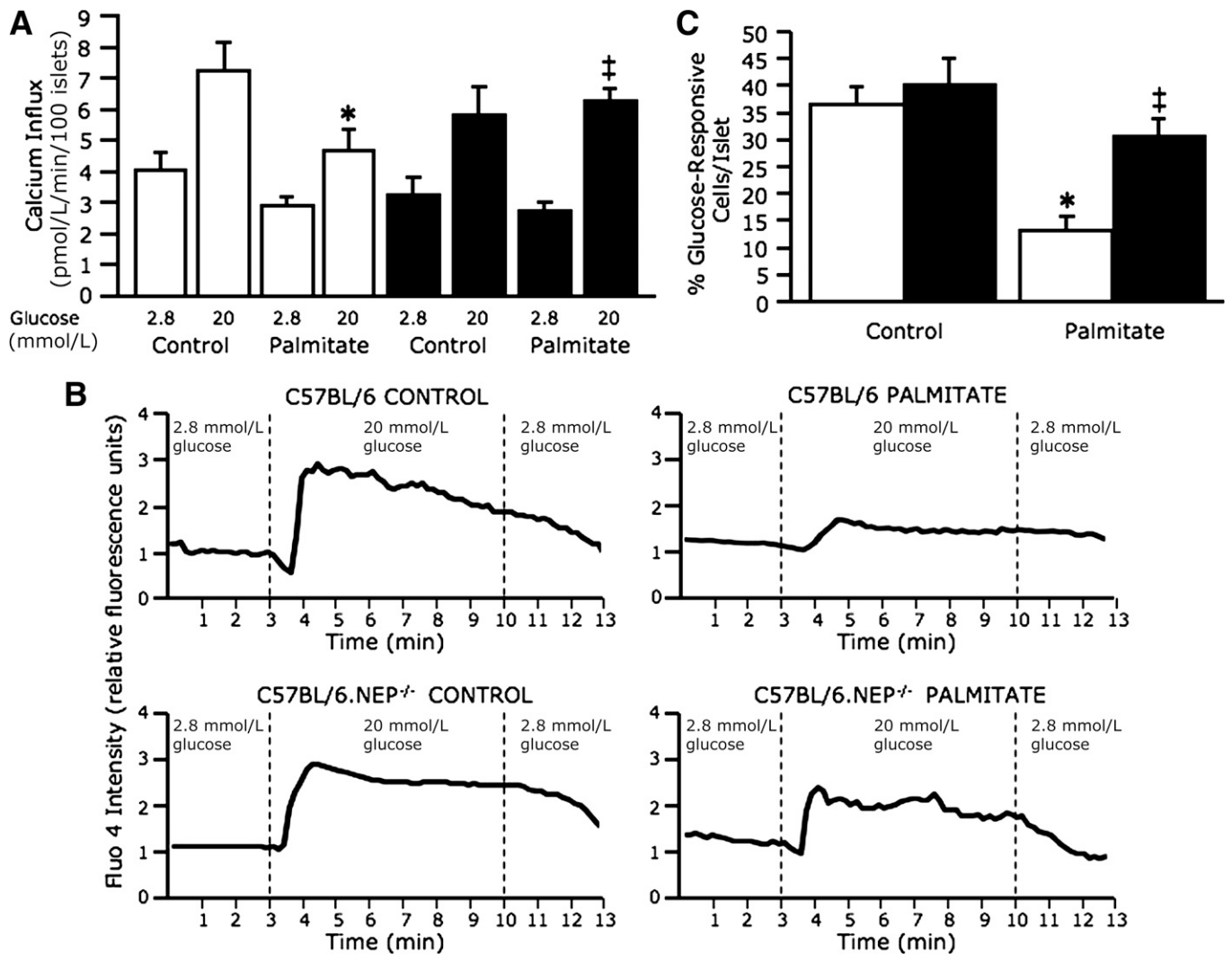


**FIG. 5.** Neprilysin-deficient islets exposed to palmitate are protected against reduced glucose-stimulated calcium influx. Calcium influx, measured using  $^{45}\text{Ca}^{2+}$ , in response to 2.8 and 20 mmol/L glucose stimulation from C57BL/6 and C57BL/6.NEP<sup>-/-</sup> islets after 48-h culture in the absence or presence of 1 mmol/L palmitate (**A**) ( $n = 5$ ). Representative traces for calcium imaging of islets loaded with fluo-4 and perfused with 2.8 mmol/L and 20 mmol/L glucose (**B**). Percentage of 20 mmol/L glucose-responsive cells per C57BL/6 or C57BL/6.NEP<sup>-/-</sup> islet after 48-h culture in the absence or presence of 1 mmol/L palmitate (**C**) ( $n = 11$ – $14$  islets/group), determined as increased fluo-4 emission intensity when the perfusion solution was switched from 2.8 to 20 mmol/L glucose. White bars, C57BL/6 islets; black bars, C57BL/6.NEP<sup>-/-</sup> islets. Data are means  $\pm$  SEM. \* $P < 0.01$  vs. control; ‡ $P < 0.05$  vs. C57BL/6.

$\beta$ -cell dysfunction. To definitively link increased neprilysin activity to decreased GSIS, we overexpressed neprilysin in C57BL/6 islets and assessed secretion after culture in the absence of palmitate. In line with the effect of palmitate to increase neprilysin activity and decrease GSIS, overexpression of neprilysin in the absence of palmitate reproduced the insulin secretion defect in response to glucose stimulation. Interestingly, overexpression of neprilysin did not alter basal insulin secretion or insulin content compared with islets infected with a control (AdV-GFP) adenovirus. This is in contrast to C57BL/6 islets cultured with palmitate, where basal insulin secretion was elevated and insulin content reduced compared with islets cultured without palmitate. With respect to this difference in basal insulin secretion, prolonged exposure to FFAs causes marked triglyceride deposition that at low glucose is associated with reduced malonyl-CoA content, an increased rate of fat oxidation (41), and thereby elevated insulin secretion. Such effects would not be expected in

AdV-NEP-infected islets cultured without palmitate. When it is also considered that in neprilysin-deficient islets cultured with palmitate basal insulin secretion and insulin content were not normalized, collectively these findings indicate that increased neprilysin activity does not modulate basal insulin secretion or insulin content but, rather, specifically affects GSIS.

The mechanism by which neprilysin reduces GSIS after prolonged FFA exposure involves reduced calcium influx, since in neprilysin-deficient islets all defects except reduced calcium influx were observed with palmitate exposure, yet GSIS was not impaired. Further, AdV-NEP-infected islets cultured in the absence of palmitate showed defects in both calcium influx and GSIS. Calcium influx through voltage-gated calcium channels serves as a critical signal to trigger insulin exocytosis with calcium channel regulation requiring a number of accessory proteins. Neprilysin may play such a role to modulate calcium influx in  $\beta$ -cells. In fact, neprilysin has been shown to modulate calcium flux in lung

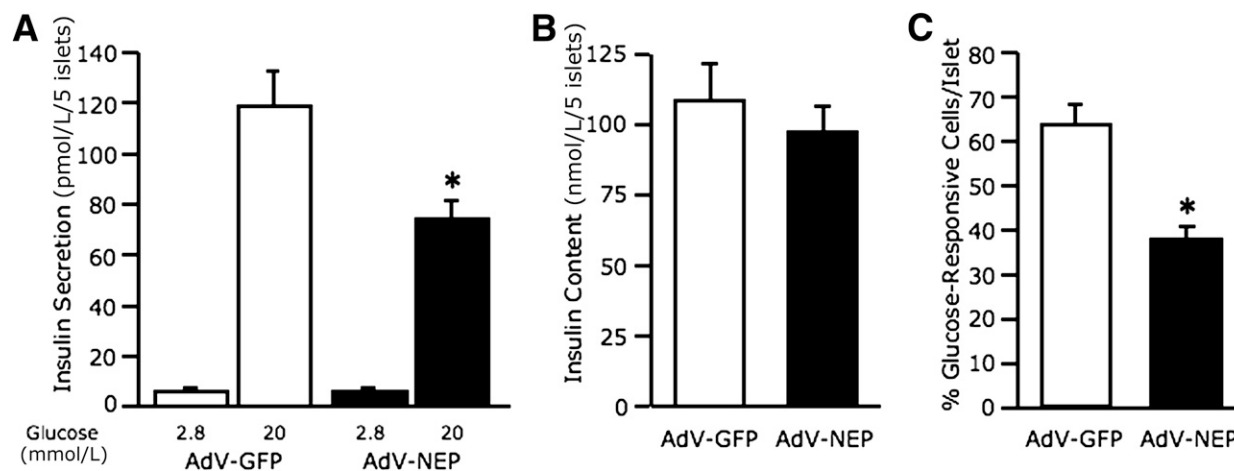


**FIG. 6.** Adenovirus-mediated upregulation of neprilysin recapitulates the impairment in GSIS and calcium influx due to palmitate exposure. Insulin secretion in response to 2.8 and 20 mmol/L glucose (*A*) ( $n = 8$ ) and islet insulin content (*B*) ( $n = 8$ ) from C57BL/6 islets after infection with either AdV-GFP or AdV-NEP and culture for 48 h in the absence of palmitate. Percentage of 20 mmol/L glucose-responsive cells per AdV-GFP or AdV-NEP islet after 48-h culture in the absence of 1 mmol/L palmitate (*C*) ( $n = 13$ – $18$  islets/group), determined as increased Rhod-3 emission intensity when the perfusion solution was switched from 2.8 to 20 mmol/L glucose. White bars, AdV-GFP; black bars, AdV-NEP. Data are means  $\pm$  SEM. \* $P < 0.02$  vs. AdV-GFP.

cells where recombinant neprilysin abolished, and neprilysin inhibition potentiated, calcium flux generated by neuropeptides (36). A similar role for neprilysin in  $\beta$ -cells would significantly impact insulin secretion. Further, the plasma membrane localization of neprilysin makes its potential interaction with calcium channels and/or accessory proteins that facilitate calcium influx plausible. Of note, neprilysin localization may explain why its ablation does not protect against FFA-induced reductions in insulin pre-mRNA and ATP levels and oxidative/nitrative stress.

As neprilysin-deficient islets cultured with palmitate did not exhibit reduced glucose-mediated calcium influx despite reduced ATP levels,  $K_{ATP}$  channel-independent mechanisms may be involved in maintaining GSIS. Perhaps the absence of neprilysin enables a key palmitate-derived mediator of  $K_{ATP}$  channel-independent glucose action to facilitate calcium influx. It is noteworthy that compared with  $K_{ATP}$  channel-dependent insulin secretion, the glucose dose response curve for  $K_{ATP}$  channel-independent insulin secretion is left shifted (42), suggesting that the metabolic threshold (including ATP requirements) for secretion is lower. This would fit with the ability of neprilysin-deficient islets cultured with palmitate to secrete comparable levels of insulin upon glucose stimulation relative to C57BL/6 islets cultured without palmitate, despite lower ATP levels.

As neprilysin can exert effects via its dual activities—proteolysis (21) or protein binding (22–24)—it may possibly either cleave and/or directly bind the cellular component(s), or perhaps even calcium channel subunits, required for calcium influx. In support of a proteolytic role, neprilysin is known to cleave the  $\alpha$ -subunit of Na,K-ATPase (37), the principal pump responsible for restoring equilibrium of  $Na^+$  and  $K^+$  ions across islet cell plasma membranes. A protein-binding role for islet neprilysin is supported by studies demonstrating that it directly binds proteins like PTEN (43) and the p110 subunit of phosphatidylinositol 3-kinase (23), which are involved in signaling pathways that alter hormone secretion (44,45) and modulate membrane ion channel activity (46,47). Whether neprilysin exerts a proteolytic or protein-binding function to mediate  $\beta$ -cell dysfunction will be the focus of future studies.

To evaluate the significance of our in vitro findings in an in vivo setting, we studied C57BL/6.NEP<sup>-/-</sup> and C57BL/6 mice after 12 weeks of high-fat feeding. Consistent with previous studies, C57BL/6 mice developed fasting hyperglycemia, fasting hyperinsulinemia, and impaired GSIS after a high-fat diet (38,39). C57BL/6.NEP<sup>-/-</sup> mice also developed fasting hyperglycemia and hyperinsulinemia but, in contrast, did not display reduced GSIS after a high-fat diet. This latter finding agrees with the in vitro data and strengthens the notion that neprilysin may be a critical mediator of fat-induced insulin secretory dysfunction. What remains in question, however, is why C57BL/6.NEP<sup>-/-</sup> mice exhibited fasting hyperglycemia despite no defect in GSIS. One potential explanation may be that since deletion of neprilysin in C57BL/6.NEP<sup>-/-</sup> mice is global, the absence of neprilysin in liver and peripheral tissues may be altering hepatic glucose production and/or peripheral insulin sensitivity, thereby impacting glycemia. That said, our IPITT data suggest that there is no effect of neprilysin deficiency on whole-body insulin action. While mice fed a high-fat diet were insulin resistant compared with mice fed a low-fat diet, insulin sensitivity did not differ between C57BL/6.NEP<sup>-/-</sup> and C57BL/6 mice. Mice fed a high-fat diet also had higher glucose levels during the IVGTT, but glucose disappearance (tolerance) was not affected by neprilysin deficiency. Our finding that neprilysin deficiency does not confer protection against all fat-induced metabolic defects is consistent with others in the literature (35,48). Importantly, it is not possible to ascertain whether other studies involving C57BL/6.NEP<sup>-/-</sup> mice also show protection against fat-induced reductions in GSIS, since only glucose but not insulin data are reported. Notwithstanding, our findings may be relevant for obese humans with type 2 diabetes. In fact, a human study showed that plasma neprilysin activity was positively correlated with BMI and measures of insulin resistance (35). Taken together with our findings, these data would suggest that inhibition of neprilysin under conditions of chronically elevated fat could be beneficial.

In summary, we demonstrate that islet neprilysin is upregulated under conditions of chronically elevated fat, which contributes to impaired GSIS. While neprilysin



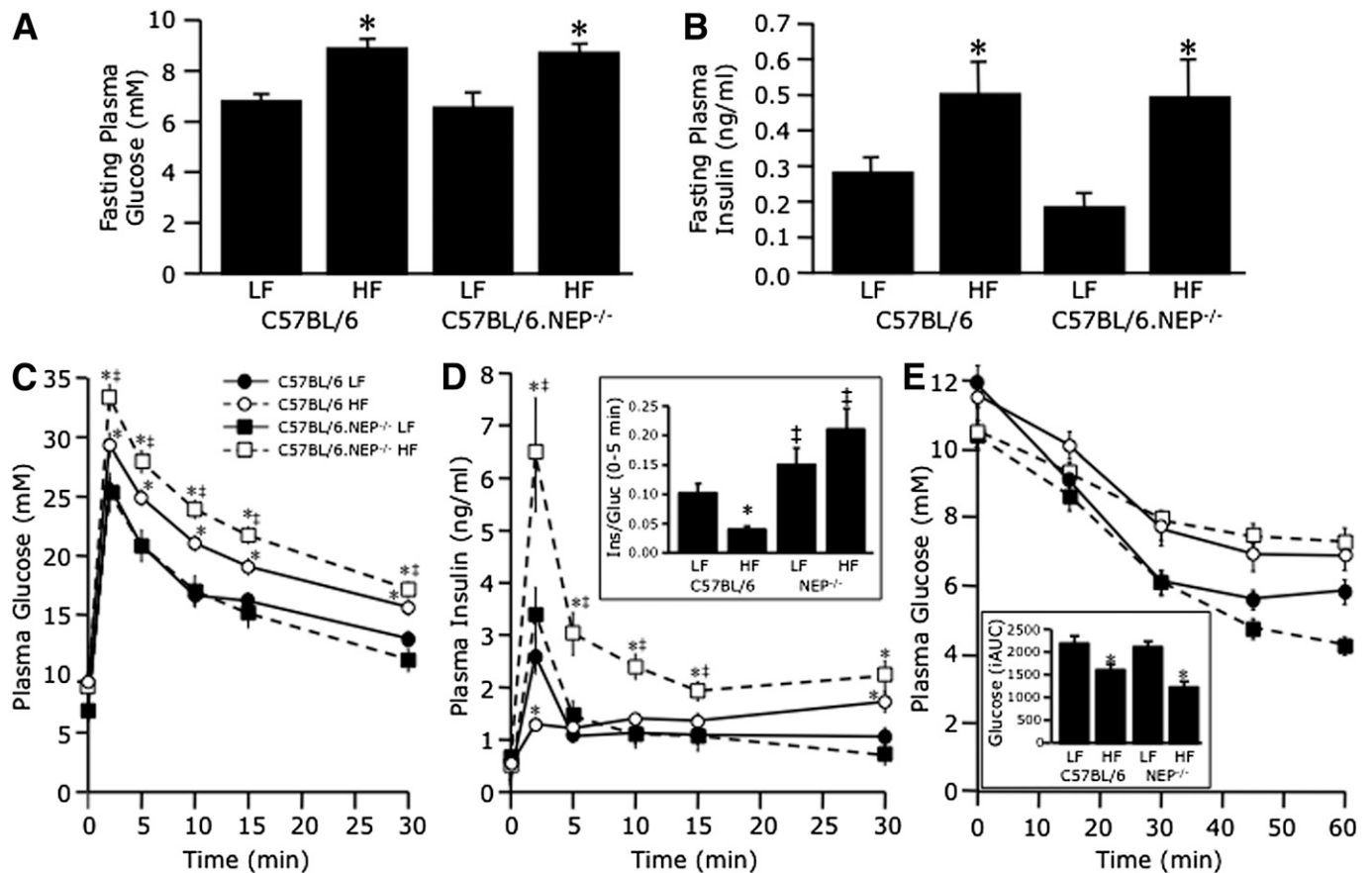


**FIG. 7.** Neprilysin-deficient mice are protected against high-fat diet-induced insulin secretory dysfunction. Fasting plasma glucose (A) and insulin (B) levels and plasma glucose (C) and insulin (D) levels in response to intravenous glucose and plasma glucose levels in response to intraperitoneal insulin (E) in C57BL/6 and C57BL/6.NEP<sup>-/-</sup> mice after 12 weeks on a low-fat (LF) or high-fat (HF) diet. The inset in D shows the early insulin response to intravenous glucose calculated as a ratio of the incremental areas under the insulin and glucose curves over the first 5 min. The inset in E shows the inverse area under the curve below baseline glucose after insulin administration. Closed circles, C57BL/6 LF; open circles, C57BL/6 high fat; closed squares, C57BL/6.NEP<sup>-/-</sup> low fat; open squares, C57BL/6.NEP<sup>-/-</sup> high fat. Data are means  $\pm$  SEM;  $n = 14$ –18. \* $P < 0.05$  vs. LF; † $P < 0.05$  vs. C57BL/6.

deficiency does not prevent many of the  $\beta$ -cell defects typically observed with chronic FFA exposure like reduced ATP levels and oxidative/nitrative stress, it protects against reductions in calcium influx and impaired GSIS. Our findings highlight the critical nature of calcium signaling for normal insulin secretion and that interventions targeted to the site of calcium influx, such as neprilysin inhibition, may improve  $\beta$ -cell function in metabolically altered states.

#### ACKNOWLEDGMENTS

This study was supported by National Institutes of Health (NIH) Grant DK-080945 (to S.Z.), the Department of Veterans Affairs, VA Puget Sound Health Care System, the Diabetes Australia Research Trust, and the National Health and Medical Research Council (NHMRC) of Australia. Calcium influx and rubidium efflux studies as well as histological studies were performed at the University of Washington's Diabetes Research Center Cell Function Analysis Core and Cellular and Molecular Imaging Core, respectively, both of which are supported by NIH Grant DK-017047. S.A. was the recipient of a Career Development Award from the NHMRC of Australia.

No potential conflicts of interest relevant to this article were reported.

S.Z. conceived and designed the study, performed experiments, analyzed data, and wrote the manuscript. D.-S.K. performed experiments and edited the manuscript.

B.M.B. performed experiments, analyzed data, and edited the manuscript. B.L. contributed the C57BL/6.NEP<sup>-/-</sup> mice. S.E.K. analyzed data and edited the manuscript. S.A. performed experiments, analyzed data, and edited the manuscript. S.Z. is the guarantor of this work and, as such, had full access to all the data in the study and takes responsibility for the integrity of the data and the accuracy of the data analysis.

The authors thank P. Bergquist, C. Braddock, M. Cone, C. Forsyth, J. Langworthy, M. Peters, M. Watts, and J. Willard from the Seattle Institute for Biomedical and Clinical Research, and A. Blair and C. Rantza from the University of Melbourne for excellent technical support.

#### REFERENCES

1. Kahn SE, Zraika S, Utzschneider KM, Hull RL. The beta cell lesion in type 2 diabetes: there has to be a primary functional abnormality. *Diabetologia* 2009;52:1003–1012
2. Frazee E, Donner CC, Swislocki AL, Chiou YA, Chen YD, Reaven GM. Ambient plasma free fatty acid concentrations in noninsulin-dependent diabetes mellitus: evidence for insulin resistance. *J Clin Endocrinol Metab* 1985;61:807–811
3. Cressin SR, Greenough WB 3rd, Steinberg D. Stimulation of insulin secretion by long-chain free fatty acids. A direct pancreatic effect. *J Clin Invest* 1973;52:1979–1984
4. Warnotte C, Gilon P, Nenquin M, Henquin JC. Mechanism of the stimulation of insulin release by saturated fatty acids. A study of palmitate effects in mouse beta-cells. *Diabetes* 1994;43:703–711

5. Sako Y, Grill VE. A 48-hour lipid infusion in the rat time-dependently inhibits glucose-induced insulin secretion and B cell oxidation through a process likely coupled to fatty acid oxidation. *Endocrinology* 1990;127:1580–1589
6. Zhou Y-P, Grill VE. Long-term exposure of rat pancreatic islets to fatty acids inhibits glucose-induced insulin secretion and biosynthesis through a glucose fatty acid cycle. *J Clin Invest* 1994;93:870–876
7. Campbell PJ, Carlson MG, Nurjhan N. Fat metabolism in human obesity. *Am J Physiol* 1994;266:E600–E605
8. Kelpe CL, Moore PC, Parazzoli SD, Wicksteed B, Rhodes CJ, Poirout V. Palmitate inhibition of insulin gene expression is mediated at the transcriptional level via ceramide synthesis. *J Biol Chem* 2003;278:30015–30021
9. Prentki M, Joly E, El-Assaad W, Roduit R. Malonyl-CoA signaling, lipid partitioning, and glucolipotoxicity: role in beta-cell adaptation and failure in the etiology of diabetes. *Diabetes* 2002;51(Suppl 3):S405–S413
10. Patanè G, Anello M, Piro S, Vigneri R, Purrello F, Rabuazzo AM. Role of ATP production and uncoupling protein-2 in the insulin secretory defect induced by chronic exposure to high glucose or free fatty acids and effects of peroxisome proliferator-activated receptor-gamma inhibition. *Diabetes* 2002;51:2749–2756
11. Carlsson C, Borg LA, Welsh N. Sodium palmitate induces partial mitochondrial uncoupling and reactive oxygen species in rat pancreatic islets in vitro. *Endocrinology* 1999;140:3422–3428
12. Shimabukuro M, Ohneda M, Lee Y, Unger RH. Role of nitric oxide in obesity-induced beta cell disease. *J Clin Invest* 1997;100:290–295
13. Collins SC, Hoppa MB, Walker JN, et al. Progression of diet-induced diabetes in C57BL/6J mice involves functional dissociation of Ca<sup>2+</sup> channels from secretory vesicles. *Diabetes* 2010;59:1192–1201
14. Gwiazda KS, Yang TL, Lin Y, Johnson JD. Effects of palmitate on ER and cytosolic Ca<sup>2+</sup> homeostasis in beta-cells. *Am J Physiol Endocrinol Metab* 2009;296:E690–E701
15. Chan CB, MacPhail RM, Sheu L, Wheeler MB, Gaisano HY. Beta-cell hypertrophy in fa/fa rats is associated with basal glucose hypersensitivity and reduced SNARE protein expression. *Diabetes* 1999;48:997–1005
16. Zraika S, Dunlop ME, Proietto J, Andrikopoulos S. Elevated SNAP-25 is associated with fatty acid-induced impairment of mouse islet function. *Biochem Biophys Res Commun* 2004;317:472–477
17. Antezana M, Sullivan SR, Usui M, et al. Neutral endopeptidase activity is increased in the skin of subjects with diabetic ulcers. *J Invest Dermatol* 2002;119:1400–1404
18. Muangman P, Spenny ML, Tamura RN, Gibran NS. Fatty acids and glucose increase neutral endopeptidase activity in human microvascular endothelial cells. *Shock* 2003;19:508–512
19. Spenny ML, Muangman P, Sullivan SR, et al. Neutral endopeptidase inhibition in diabetic wound repair. *Wound Repair Regen* 2002;10:295–301
20. Zraika S, Hull RL, Udayasankar J, et al. Identification of the amyloid-degrading enzyme neprilysin in mouse islets and potential role in islet amyloidogenesis. *Diabetes* 2007;56:304–310
21. Turner AJ, Tanzawa K. Mammalian membrane metalloproteinases: NEP, ECE, KELL, and PEX. *FASEB J* 1997;11:355–364
22. Ganju RK, Shpektor RG, Brenner DG, Shipp MA. CD10/neutral endopeptidase 24.11 is phosphorylated by casein kinase II and coassociates with other phosphoproteins including the lyn src-related kinase. *Blood* 1996;88:4159–4165
23. Shen R, Milowsky MI, Ozaki N, et al. Detection of the p110 beta subunit of phosphatidylinositol 3-kinase complexed with neutral endopeptidase. *Anticancer Res* 2002;22:2533–2538
24. Sumitomo M, Shen R, Walburg M, et al. Neutral endopeptidase inhibits prostate cancer cell migration by blocking focal adhesion kinase signaling. *J Clin Invest* 2000;106:1399–1407
25. Turner AJ, Isaac RE, Coates D. The neprilysin (NEP) family of zinc metalloproteinases: genomics and function. *Bioessays* 2001;23:261–269
26. Sumitomo M, Milowsky MI, Shen R, et al. Neutral endopeptidase inhibits neuropeptide-mediated transactivation of the insulin-like growth factor receptor-Akt cell survival pathway. *Cancer Res* 2001;61:3294–3298
27. Hupe-Sodmann K, McGregor GP, Bridenbaugh R, et al. Characterisation of the processing by human neutral endopeptidase 24.11 of GLP-1(7-36) amide and comparison of the substrate specificity of the enzyme for other glucagon-like peptides. *Regul Pept* 1995;58:149–156
28. Zraika S, Aston-Mourney K, Marek P, et al. Neprilysin impedes amyloid formation by inhibition of fibril formation rather than peptide degradation. *J Biol Chem* 2010;285:18177–18183
29. Gafford JT, Skidgel RA, Erdös EG, Hersh LB. Human kidney “enkephalinase”, a neutral metalloendopeptidase that cleaves active peptides. *Biochemistry* 1983;22:3265–3271
30. Yamamoto K, Chappell MC, Brosnihan KB, Ferrario CM. In vivo metabolism of angiotensin I by neutral endopeptidase (EC 3.4.24.11) in spontaneously hypertensive rats. *Hypertension* 1992;19:692–696
31. Lu B, Gerard NP, Kolakowski LF Jr, et al. Neutral endopeptidase modulation of septic shock. *J Exp Med* 1995;181:2271–2275
32. Zraika S, Dunlop M, Proietto J, Andrikopoulos S. The hexosamine biosynthesis pathway regulates insulin secretion via protein glycosylation in mouse islets. *Arch Biochem Biophys* 2002;405:275–279
33. Jung SR, Reed BJ, Sweet IR. A highly energetic process couples calcium influx through L-type calcium channels to insulin secretion in pancreatic beta-cells. *Am J Physiol Endocrinol Metab* 2009;297:E717–E727
34. Koopitwut S, Zraika S, Thorburn AW, et al. Comparison of insulin secretory function in two mouse models with different susceptibility to beta-cell failure. *Endocrinology* 2002;143:2085–2092
35. Standeven KF, Hess K, Carter AM, et al. Neprilysin, obesity and the metabolic syndrome. *Int J Obes (Lond)* 2011;35:1031–1040
36. Cohen AJ, Bunn PA, Franklin W, et al. Neutral endopeptidase: variable expression in human lung, inactivation in lung cancer, and modulation of peptide-induced calcium flux. *Cancer Res* 1996;56:831–839
37. Groubman MA, Kamanina YV, Petrushanko Iu, Rubtsov AM, Lopina OD. Neutral endopeptidase neprilysin is copurified with Na,K-ATPase from rabbit outer medulla and hydrolyzes its  $\alpha$ -subunit. *Biochemistry (Mosc)* 2010;75:1281–1284
38. Reimer MK, Ahrén B. Altered beta-cell distribution of pdx-1 and GLUT-2 after a short-term challenge with a high-fat diet in C57BL/6J mice. *Diabetes* 2002;51(Suppl. 1):S138–S143
39. Surwit RS, Kuhn CM, Cochrane C, McCubbin JA, Feinglos MN. Diet-induced type II diabetes in C57BL/6J mice. *Diabetes* 1988;37:1163–1167
40. Zraika S, Dunlop M, Proietto J, Andrikopoulos S. Effects of free fatty acids on insulin secretion in obesity. *Obes Rev* 2002;3:103–112
41. Segall L, Lameloise N, Assimacopoulos-Jeannet F, et al. Lipid rather than glucose metabolism is implicated in altered insulin secretion caused by oleate in INS-1 cells. *Am J Physiol* 1999;277:E521–E528
42. Asanuma N, Aizawa T, Sato Y, et al. Two signaling pathways, from the upper glycolytic flux and from the mitochondria, converge to potentiate insulin release. *Endocrinology* 1997;138:751–755
43. Sumitomo M, Iwase A, Zheng R, et al. Synergy in tumor suppression by direct interaction of neutral endopeptidase with PTEN. *Cancer Cell* 2004;5:67–78
44. Nunoi K, Yasuda K, Tanaka H, et al. Wortmannin, a PI3-kinase inhibitor: promoting effect on insulin secretion from pancreatic beta cells through a cAMP-dependent pathway. *Biochem Biophys Res Commun* 2000;270:798–805
45. Wang L, Liu Y, Yan Lu S, et al. Deletion of Pten in pancreatic  $\beta$ -cells protects against deficient  $\beta$ -cell mass and function in mouse models of type 2 diabetes. *Diabetes* 2010;59:3117–3126
46. El-Kholy W, Macdonald PE, Lin JH, et al. The phosphatidylinositol 3-kinase inhibitor LY294002 potently blocks K(V) currents via a direct mechanism. *FASEB J* 2003;17:720–722
47. Khan FA, Goforth PB, Zhang M, Satin LS. Insulin activates ATP-sensitive K(+) channels in pancreatic beta-cells through a phosphatidylinositol 3-kinase-dependent pathway. *Diabetes* 2001;50:2192–2198
48. Davidson E, Coppey L, Lu B, Arballo V, Calcutt NA, Gerard C, Yorek M. The roles of streptozotocin neurotoxicity and neutral endopeptidase in murine experimental diabetic neuropathy. *Exp Diabetes Res* 2009;2009:431980